Shear-Induced Chiral Migration of Particles with Anisotropic Rigidity

Nobuhiko Watari*
Macromolecular Science and Engineering Center, University of Michigan, Ann Arbor, Michigan 48109-2136, USA

Ronald G. Larson
Department of Chemical Engineering, Macromolecular Science and Engineering Center, University of Michigan, Ann Arbor, Michigan 48109-2136, USA
(Received 5 March 2009; published 16 June 2009)

We report that an achiral particle with anisotropic rigidity can migrate in the vorticity direction in shear flow. A minimal ''tetrumbbell'' model of such a particle is constructed from four beads and six springs to make a tetrahedral structure. A combination of two different spring constants corresponding to ''hard'' and ''soft'' springs yields ten distinguishable tetrumbbells, which when simulated in shear flow with hydrodynamic interactions between beads but no Brownian motion at zero Reynolds number, produces five different types of behavior in which seven out of ten tetrumbbell structures migrate in the vorticity direction due to shear-induced chirality. Some of the structures migrate in the same direction along the vorticity direction even when the shear flow is reversed, which is impossible for permanently chiral objects.

DOI: 10.1103/PhysRevLett.102.246001 PACS numbers: 83.50.−v, 05.60.Cd, 47.85.Np

Microscopic biological objects, including cells, often have complex and anisotropic internal structures. The mechanical response of such an object to an external field will differ significantly from that of an object with uniform internal structure. Although the dynamics in flows of rigid particles with axisymmetric or chiral shape [1–5] and of flexible particles or droplets with isotropic mechanical properties [6–8] have been studied, there has been very little investigation of the effect of *anisotropic structure* or rigidity on the dynamics of a deformable particle in a flow. Here, we therefore develop a very simple model of an achiral particle with anisotropic rigidity and show by computer simulations that in a shear flow at vanishing Reynolds number it can deform into chiral shape and migrate in the vorticity direction.

Fundamental studies of the dynamics of deformable objects, such as polymer molecules, have long been conducted using simple dumbbell, trumbbell, and multispring models with minimal degrees of freedom [9–11]. A minimal model of a deformable object with three-dimensional anisotropic structure is a tetrahedron containing four beads and six springs, which we call ''tetrumbbell'' (see Fig. 1). Each of the six springs is a ''FENE-Fraenkel (FF) spring'' [12] with the same equilibrium length L but different spring constant k, and its deformed spring length Q is restricted to a range set by the parameter s:

$$\boldsymbol{f}^{\mathrm{FF}} = k\frac{Q-L}{1-(1-Q/L)^2/s^2}\frac{\boldsymbol{Q}}{Q} \quad \text{for } (1-s) < Q/L < (1+s). \quad (1)$$

The FF spring avoids overlaps of beads or springs, which would be unavoidable with Hookean springs under a strong external flow. Note that the shape of the tetrumbbell is achiral in equilibrium (i.e., it is a regular tetrahedron), since all beads have identical hydrodynamic radius and all springs have identical equilibrium length.

The shear-induced motion of a tetrumbbell is computed according to the following discretized differential equation for each bead:

$$\boldsymbol{r}_i(t+\Delta t) = \boldsymbol{r}_i(t) + \left\{\boldsymbol{v}_{\mathrm{flow}}(\boldsymbol{r}_i) + \sum_{j=1}^{4}\mathcal{H}_{ij}\cdot\boldsymbol{f}_j\right\}\Delta t, \quad (2)$$

where $\boldsymbol{r}_i(t)$ is the position of bead i $(=1,2,3,4)$ at time t, $\boldsymbol{f}_i$ is the summation of the FF spring forces on bead i, and the flow velocity field $\boldsymbol{v}_{\mathrm{flow}}$ is $\boldsymbol{v}_{\mathrm{flow}}(\boldsymbol{r}) = \dot{\gamma}_{xy} r_y \boldsymbol{e}_x$ with $\dot{\gamma}_{xy}$ and $\boldsymbol{e}_x$ being the shear rate and the unit vector in the x direction, respectively. $\mathcal{H}_{ij}$ is the Rotne-Prager-Yamakawa hydrodynamic interaction tensor [11,13,14] given by

$$\mathcal{H}_{ii} = \frac{1}{6\pi\eta a}\boldsymbol{I}, \quad (3)$$

$$\mathcal{H}_{ij} = \frac{1}{8\pi\eta r_{ij}}\left[\left(1+\frac{2a^2}{3r_{ij}^2}\right)\boldsymbol{I} + \left(1-\frac{2a^2}{r_{ij}^2}\right)\frac{\boldsymbol{r}_{ij}\boldsymbol{r}_{ij}}{r_{ij}^2}\right] \quad \text{if } i \neq j \text{ and } r_{ij} \geq 2a, \quad (4)$$

$$\mathcal{H}_{ij} = \frac{1}{6\pi\eta a}\left[\left(1-\frac{9r_{ij}}{32a}\right)\boldsymbol{I} + \frac{3}{32}\frac{\boldsymbol{r}_{ij}\boldsymbol{r}_{ij}}{a r_{ij}}\right] \quad \text{if } i \neq j \text{ and } r_{ij} < 2a. \quad (5)$$

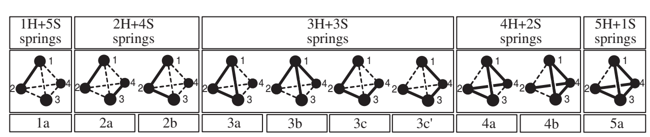

FIG. 1. The ten distinguishable tetrumbbell structures constructed from four beads and six springs, each of which is either a hard (H, solid line) or soft (S, dotted line) spring.

Here, $\boldsymbol{r}_{ij} = \boldsymbol{r}_i - \boldsymbol{r}_j$, $\mathcal{I}$ is the 3×3 identity matrix, and a is the bead radius. Using this model, we compute the response of a tetrumbbell to shear taking into account its hydrodynamic interactions through solvent motion. Brownian motion and inertia are both neglected in this study. Nevertheless, the dynamics of the tetrumbbell is not time reversible due to two sources of nonlinearity, namely, the nonlinearity of the FF spring force and the nonlinearity that arises from the finite relaxation time of the deformation of the tetrumbbell.

The model has three input parameters with physical units: a (bead radius), η (solvent viscosity), and k (typical FF spring constant). Therefore, we scale length and time by a and $\tau = a\eta/k$, respectively. The dimensionless shear rate and the migration velocity in the vorticity direction are given by $\Pi_s = \dot{\gamma}_{xy}\eta a/k$ and $\Pi_{\rm vz} = V_z^{\rm cm}\eta/k$, where $V_z^{\rm cm}$ is the center-of-mass velocity of the tetrumbbell in the vorticity direction.

The spring parameters (k_n, s_n), where n is spring index $(n = 1, 2, \ldots, 6)$, are chosen to be either "hard" $(k_{\rm hard}, s_{\rm hard}) = (1000k, 0.001)$ or "soft" $(k_{\rm soft}, s_{\rm soft}) = (k, 0.5)$ for simplicity, and the equilibrium length of the FF springs is set to $L = 5a$. Within these specifications, ten distinguishable structures of tetrumbbells can be constructed, which are shown in Fig. 1. Note that the structures $(3c)$ and $(3c')$ in Fig. 1 have hard backbones that possess chirality through three hard springs, but the others lack chirality in either particle or backbone shape, in the absence of flow. We computed the motion of tetrumbbells with structure $(1a), (2a), \ldots, (5a)$ in a shear flow of strength $0.002 \leq |\Pi_s| \leq 0.2$ with time step $\Delta t = 10^{-3}$, with various initial orientations of the tetrumbbell relative to the shear direction.

We find that all tetrumbbells except for $(3b)$, $(4a)$, and $(5a)$ migrate in the vorticity direction in shear flow. Five types of migration are observed:

(i) Type M: the tetrumbbell migrates in the vorticity direction and the direction of the migration (i.e., the $+z$ or $-z$ direction) depends on the initial orientation of the tetrumbbell.

(ii) Type A: the tetrumbbell migrates in the vorticity direction in shear flow only above a threshold shear rate, which is dependent on the initial orientation of the tetrumbbell, and the direction of the migration also depends on the initial orientation.

(iii) Type C: the tetrumbbell migrates in the vorticity direction and the direction of the migration does not depend on the initial orientation of the tetrumbbell.

(iv) Type N: the tetrumbbell does not migrate in the vorticity direction in shear flow.

(v) Type M/N: the tetrumbbell shows migration of either type M or N depending on the initial orientation of the tetrumbbell.

Table I shows the migration type for each tetrumbbell structure, and a typical migration history is shown in Figs. 2 and 3 in terms of the center-of-mass position, velocity, and conformation. In a steady shear flow, tetrumbbells of migration types M, C, and A deform and change their conformation and migration velocity periodically, with each cycle producing a net migration in the vorticity direction. The tetrumbbell does not migrate when the hydrodynamic interaction is turned off (i.e., $\mathcal{H}_{ij} = 0$ for $i \neq j$). It is also worth noting that the unit vector pointing from the center of mass to a specific bead of the tetrumbbell follows a closed orbit at steady state, analogous to the Jeffery orbit of a axisymmetric particle in shear flow [1]. Since a particle with achiral shape does not migrate in shear flow in the vorticity direction because of the reflection symmetry of hydrodynamics in shear flow [2], the migration of tetrumbbell can be attributed to the chiral deformation induced by the shear flow. To quantify the chirality of a tetrumbbell in motion, we introduce a chiral deflection index χ,

$$\chi = \sqrt[3]{G_0}, \tag{6}$$

$$G_0 = \frac{1}{3}\Bigg[\sum_{i,j,k,l=1\cdots4} \frac{[(\boldsymbol{r}_{ij} \times \boldsymbol{r}_{kl}) \cdot \boldsymbol{r}_{il}](\boldsymbol{r}_{ij} \cdot \boldsymbol{r}_{jk})(\boldsymbol{r}_{jk} \cdot \boldsymbol{r}_{kl})}{(r_{ij}r_{jk}r_{kl})^2 r_{il}}\Bigg]. \tag{7}$$

Here, G_0 is a chirality index proposed in Ref. [15] for molecules, and χ is the cube root of G_0, making it proportional to the shear rate $\dot{\gamma}_{xy}$ at low shear rate for tetrumbbells. The chiral deflection index differs from zero if the tetrumbbell deforms into a chiral geometry, and is invariant under rotation, translation, and dilation, but changes sign on reflection. As shown in Fig. 3, the tetrumbbell has chiral

TABLE I. Types of shear migration of different tetrumbbell structures.

Structure of tetrumbbell	$1a$	$2a$	$2b$	$3a$	$3b$	$3c$	$3c'$	$4a$	$4b$	$5a$
Migration type	A	A	M/N	M	N	C	C	N	M	N

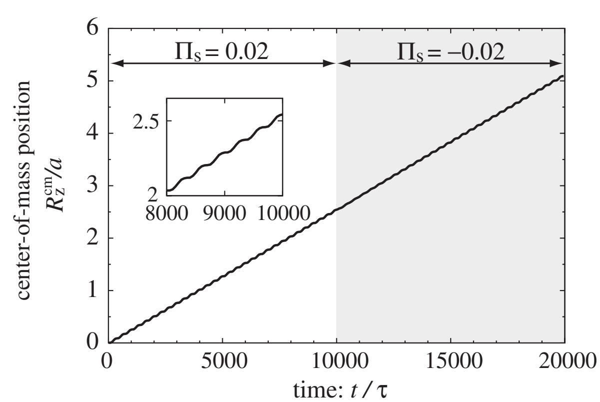

FIG. 2. History of the center-of-mass position of tetrumbbell $(2b)$ of migration type M in the vorticity direction ($R_z^{\rm cm}$). The shear rate is changed from $\Pi_s = 0.02$ to $\Pi_s = -0.02$ at time $t/\tau = 10\,000$.

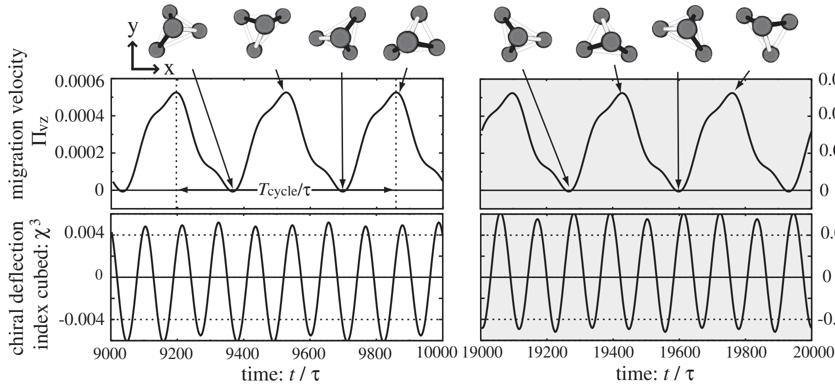

FIG. 3. History of the conformation change, the migration velocity in the vorticity direction, and the chiral deflection index of tetrumbbell ($2b$) of migration type M, which corresponds to the migration history in Fig. 2. The shear rate is $\Pi_s = 0.02$ for the plots on the left side and $\Pi_s = -0.02$ for those on the right side. The black and white bonds in the figures of the tetrumbbell conformation show the hard and soft springs, respectively. Note that the history of chiral deflection index changes sign upon reversal of the shear direction. In this case, $T_{\mathrm{cycle}}/\tau \simeq 670$.

shape in shear flow, and the instantaneous chirality induces migration in the vorticity direction.

To evaluate the migration velocity of tetrumbbells of migration types M, A, and C at steady state, the center-of-mass velocity in the vorticity direction was averaged over time for one cycle of deformation process (T_{cycle}),

$$|\Pi_{\mathrm{vz}}^{\mathrm{ave}}| = \left| \frac{1}{T_{\mathrm{cycle}}} \int_t^{t+T_{\mathrm{cycle}}} \Pi_{\mathrm{vz}}(t')dt' \right|, \tag{8}$$

and plotted in Fig. 4. From dimensional analysis, we expect $|\Pi_{\mathrm{vz}}^{\mathrm{ave}}| = \mathrm{func}(\Pi_s, s_{\mathrm{soft}}, s_{\mathrm{hard}}, k_{\mathrm{hard}}/k_{\mathrm{soft}}, L/a)$. Since we hold s_{soft}, s_{hard}, $k_{\mathrm{hard}}/k_{\mathrm{soft}}$, and L/a constant through our simulations, this simplifies to $|\Pi_{\mathrm{vz}}^{\mathrm{ave}}| = \mathrm{func}(\Pi_{\mathrm{s}})$. When the shear rate is small enough that the nonlinearity of the spring force and the effect of relaxation time of tetrumbbell deformation are not significant, the relation between $|\Pi_{\mathrm{vz}}^{\mathrm{ave}}|$ and Π_s follows a quadratic power law:

$$|\Pi_{\mathrm{vz}}^{\mathrm{ave}}| = C_{\mathrm{str}}\Pi_s^2, \tag{9}$$

or

$$|V_z^{\mathrm{cm,ave}}| = C_{\mathrm{str}}(\eta a^2/k)\dot{\gamma}_{xy}^2, \tag{10}$$

where C_{str} is a positive constant unique to each structure of tetrumbbell, and $V_z^{\mathrm{cm,ave}}$ is the time-averaged center-of-mass velocity in the vorticity direction.

In the regime $|\Pi_s| < 0.02$ where the quadratic power law holds, the stretch of the soft spring Q_{soft} is $0.85L \lesssim Q_{\mathrm{soft}} \lesssim 1.15L$, and the Weissenberg number Wi is less than 0.3, where $\mathrm{Wi} = \dot{\gamma}_{xy}\tau_{\mathrm{relax}}$ with τ_{relax} being the relaxation time of the tetrumbbell deformation [16]. Since the nonlinear effects in this regime of shear rate are small, the magnitude of the chiral deflection of the tetrumbbell is proportional to the shear rate. In general, the migration velocity of a rigid chiral object V_z^{rigid} is a product of the shear rate $\dot{\gamma}_{xy}$ and a constant g that is determined by the shape of the object [2],

$$V_z^{\mathrm{rigid}} = g\dot{\gamma}_{xy}. \tag{11}$$

Therefore, the quadratic power law for the tetrumbbell results from the proportionality between the perturbation of g and the shear rate $\dot{\gamma}_{xy}$.

In the high shear rate regime ($|\Pi_s| \gtrsim 0.02$), the quadratic power law no longer holds because the magnitude of the chiral deflection is nonlinear in the shear rate, and the time-delayed motion caused by a finite Wi becomes non-negligible. Also, the migrations type A of structures ($1a$) and ($2a$) are triggered by a nonlinear effect because the

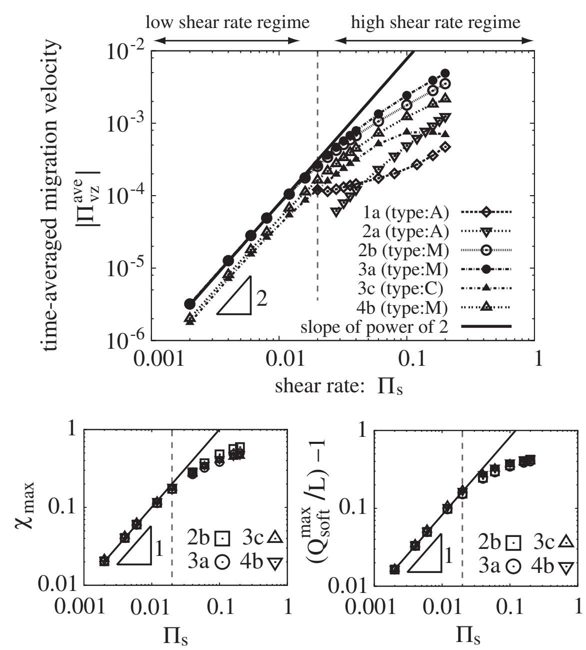

FIG. 4. (top) The time-averaged migration velocity $|\Pi_{\mathrm{vz}}^{\mathrm{ave}}|$ as a function of shear rate Π_s for each type of tetrumbbell. (bottom left) The maximum of the chiral deflection index ($\chi_{\max}$) in one cycle of deformation as a function of the shear rate. The solid line has the slope of power of 1. (bottom right) The maximum stretch ratio of soft spring $(Q_{\mathrm{soft}}^{\max} - L)/L$ in one cycle of deformation as a function of the shear rate.

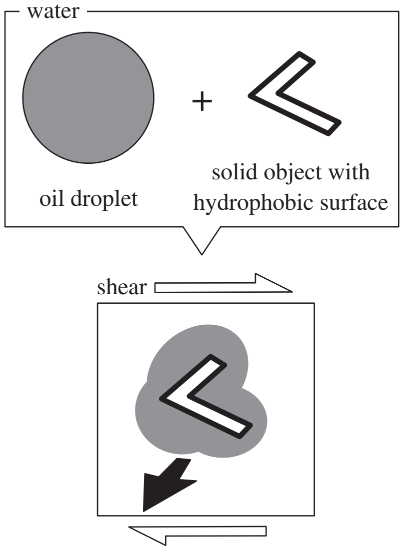

FIG. 5. Sketch of possible migration of a droplet enclosing a solid object in shear flow.

migration of type A cannot be observed at all in the low shear rate regime.

The quadratic power law, however, does not tell us the direction of migration of a tetrumbbell. Although the magnitude of the migration velocity only depends on the shear rate, the direction of migration depends on the initial orientation of the tetrumbbell except for (3c) and (3c'), which have intrinsic chirality in their backbone and always migrate in a direction that is determined by this backbone chirality. Note that the backbone chirality, by itself, does not lead to migration, since at rest the bead positions, which produce the hydrodynamic effects, are achiral. The chiral backbone does, however, determine the shear deformation of the tetrumbbell, including its shear-induced chirality.

Also, surprisingly, a switch of the shear direction from $\Pi_s = \Pi_{s0}$ to $-\Pi_{s0}$ does not necessarily change the direction of migration. Although the tetrumbbells of migration types A and C do change migration direction (i.e., from $+z$ to $-z$ direction or vice versa) upon reversal of the shear direction, the tetrumbbells of migration type M do not (see Fig. 2). This is because the tetrumbbells of migration type M change sign of the chiral deflection index upon reversal of the shear direction, but those of migration types A and C do not, as we confirmed by plotting the chiral deflection index (see Fig. 3 for type M). For a rigid chiral particle, which has an intrinsic chirality, the migration direction must change when the shear direction is reversed according to Eq. (11). The response of a tetrumbbell of migration type M to reversal of the shear direction is possible because the chirality is not intrinsic but shear induced.

Our simulation results for simple tetrumbbells show the possibility that an achiral deformable object with anisotropic rigidity can migrate in the vorticity direction in a shear flow due to shear-induced chirality. By setting the simulation parameters to be $a = 20$ [μm], $\eta = 100$ [cP], and $k = 1$ [mN/m], we find a migration velocity of 3 [μm/sec] at a shear rate of 10 [sec^{-1}] using the result of our simulation $(|\Pi_{vz}^{ave}|, \Pi_s) = (3 \times 10^{-4}, 0.02)$ in Fig. 4. In practice, migration due to the shear-induced chirality might be observed for a multiphasic particle [17,18], which has two or more distinct compartments of different elastic moduli. Another example will be an oil droplet in water under shear, if the droplet encases a solid object of comparable dimension to the droplet (see Fig. 5). An oil droplet enclosing a solid object could act as a particle with anisotropic rigidity. Depending on the shape of the solid object, the complex might migrate in the vorticity direction in a shear flow. Such a phenomenon might be used to separate small objects with polydispersity in size or shape.

We acknowledge support from NSF under Grant No. NSEC EEC-0425626.

*nobuhiko@umich.edu

[1] S. Kim and S. J. Karrila, *Microhydrodynamics: Principles and Selected Applications* (Butterworth-Heinemann, Stoneham, 1991).
[2] M. Makino and M. Doi, Phys. Fluids **17**, 103605 (2005).
[3] M. Makino, L. Arai, and M. Doi, J. Phys. Soc. Jpn. **77**, 064404 (2008).
[4] M. Kostur, M. Schindler, P. Talkner, and P. Hanggi, Phys. Rev. Lett. **96**, 014502 (2006).
[5] J. Lighthill, J. Eng. Math. **30**, 35 (1996).
[6] H. Noguchi and G. Gompper, Phys. Rev. Lett. **93**, 258102 (2004).
[7] H. A. Stone, Annu. Rev. Fluid Mech. **26**, 65 (1994).
[8] M. R. Kennedy, C. Pozrikidis, and R. Skalak, Comput. Fluids **23**, 251 (1994).
[9] R. B. Bird, C. F. Curtis, R. C. Armstrong, and O. Hassager, *Dynamics of Polymeric Liquids*, Kinetic Theory Vol. 2 (Wiley-Interscience, New York, 1987), 2nd ed.
[10] K. Nagasaka and H. Yamakawa, J. Chem. Phys. **83**, 6480 (1985).
[11] R. Jendrejack, J. J. de Pablo, and M. D. Graham, J. Chem. Phys. **116**, 7752 (2002).
[12] C. C. Hsieh, S. Jain, and R. G. Larson, J. Chem. Phys. **124**, 044911 (2006).
[13] J. Rotne and S. Prager, J. Chem. Phys. **50**, 4831 (1969).
[14] H. Yamakawa, J. Chem. Phys. **53**, 436 (1970).
[15] M. Solymosi and R. J. Low, J. Chem. Phys. **116**, 9875 (2002).
[16] The relaxation time of the tetrumbbell deformation was computed from a history of the chiral deflection index of a tetrumbbell under no flow with its initial configuration having a nonzero chiral deflection index. The history was fitted by the following equation to obtain the longest relaxation time: $\chi(t) = \chi(0) \exp(-t/\tau_{relax})$ when $\chi(t)/\chi(0) \leq 0.7$.
[17] K. H. Roh, D. C. Martin, and J. Lahann, Nature Mater. **4**, 759 (2005).
[18] K. H. Roh, D. C. Martin, and J. Lahann, J. Am. Chem. Soc. **128**, 6796 (2006).